

## Influence of Free-Field Strains on Nonlinear Lateral Abutment Stiffnesses

R. Siddharthan<sup>1</sup>, M. El-Gamal<sup>2</sup> and E. A. Maragakis<sup>3</sup>

### ABSTRACT

This paper presents an efficient approach, based on many well-established soil mechanics principles, to evaluate the nonlinear longitudinal bridge abutment spring stiffnesses. The applicability of previous studies is limited because such studies are incapable of handling many important factors such as nonlinear soil behavior, free-field strains induced by an earthquake, and the difference in soil behavior under active and passive conditions. The proposed approach accounts for all of these factors. The procedures adopted in this approach are relatively simple, and emphasis has been placed on easy interpretation and on achieving consistency between design procedures routinely used in the static and seismic design of abutments.

### INTRODUCTION

Seismic response of highway bridges can be significantly influenced by the behavior of the foundation soil that supports the abutments. Soil conditions exert a very strong influence on the seismic behavior of highway bridges. In the cases of skew bridges and short span bridges, the influence of "bridge-abutment-backfill" interaction often has a first-order effect on the overall dynamic response. Analytical studies, which are needed to evaluate the adequacy of designs, require characterization of the support at the abutments. The current procedure (e.g., AASHTO, 1983 and CalTrans) is to specify equivalent linear spring coefficients at the deck-abutment support. Many field observations (e.g., downhole array measurements) and seismological data from earthquakes have revealed that soil exhibits nonlinear behavior in strong motion earthquakes (Yu et al., 1993). An excitation with a maximum acceleration,  $a_{max}$ , of around 0.1g is strong enough to require nonlinear characterization for soils. The study reported here is concerned with the development of a nonlinear force-displacement (or stiffness) under longitudinal loading conditions for use in abutment modeling. Only seat-type abutments resting on spread footing is addressed in this paper.

Past studies to evaluate abutment stiffness values have been based on many assumptions that

---

<sup>I</sup>Associate Professor, Dept. of Civil Engineering, University of Nevada, Reno, NV 89557

<sup>II</sup>Graduate Student, Dept. of Civil Engineering, University of Nevada, Reno, NV 89557

<sup>III</sup>Professor, Dept. of Civil Engineering, University of Nevada, Reno, NV 89557

are not quite realistic (Maragakis and Siddharthan, 1989; Wilson and Tan, 1990; ATC, 1978) and, therefore, suffer from many, often serious, limitations. For example, these methods ignore one or more of the following important factors: nonlinear soil behavior, earthquake induced strains (i.e., free-field strains), the presence of active and passive conditions and the corresponding difference in soil behavior under such loading, influence of wing walls, and physical abutment dimensions.

## PROPOSED METHODOLOGY

Figure 1 shows a sketch of a displaced abutment caused by a horizontal force,  $P_L$  applied to the abutment. To find secant abutment stiffness, it is required to find the force required to cause a certain horizontal displacement ( $\delta_L$ ). The force and the displacement should be monitored near the top of the abutment since the abutment springs are assumed to be located at the bridge deck level. The movement of the abutment suggests that active and passive conditions develop in front and at the back of the abutment as shown in Fig. 1. At the bottom of the abutment, there is rotation resulting in increase and decrease in foundation pressures as shown in the figure. A close look at the figure suggests that, to estimate the force  $P_L$  for a given  $\delta_L$ , one needs the characterization of (1) the wall movement/lateral earth pressure relationship under active and passive conditions, (2) the rotational resistive moment/rotation relationship, and (3) foundation-soil interface forces (horizontal and vertical) at the bottom of the abutment.

By resolving forces in the vertical direction and taking moments about the center of the abutment base, it is possible to find the force,  $P_L$ , required to cause a certain displacement,  $\delta_L$ . The proposed numerical procedure results in abutment rotation,  $\theta$ , and  $P_L$  as solutions after satisfying all of the conditions of equilibrium (force and moment).

### Lateral Wall Movement/Earth Pressure Relationship

The earth pressure that acts on a wall vary with wall displacement. Laboratory measurements and finite element studies have shown that the active conditions in a soil deposit can be mobilized with a much lower wall movement/wall height ratio ( $\Delta/h$ ) than can the passive conditions. For medium sand, the  $\Delta/h$  ratio for the passive conditions can be as much as ten times that needed for the active condition. Figure 2 shows a range for wall movement/lateral earth pressure relationships reported for medium dense sand by Clough and Duncan (1991). The top curve is for fully compacted soil behind a non-yielding wall, and the bottom curve is for soils with no compaction. The average curve shown in Fig. 2 was selected to represent the active and passive pressure-wall displacement relationship.

### Resistive Moment-Rotation Relationship at Abutment Base

Using a Winkler spring representation for soil, Siddharthan et al. (1992), recently presented a procedure to obtain foundation resistive moment,  $M_D$ , for a rectangular spread footing (Fig. 3). They considered two important aspects: the foundation pressure should not exceed the ultimate bearing pressure and lifting off of foundation. They showed that, depending on the value of the vertical component of the force,  $F_v$ , the foundation could first reach ultimate bearing capacity (right corner) and then subsequently lift off (Case A) or vice versa (Case B). Case A occurs when  $F_v \geq$

$q_{ult}B/2$  in which  $q_{ult}$  is the bearing capacity of the foundation soil. The moment/rotation relationship depends on the ultimate bearing pressure,  $q_{ult}$ ,  $F_v$  and the Winkler spring constant,  $K_v$ . The  $K_v$ , which is stress-dependent, can, in turn, be evaluated from the vertical load-displacement ( $F_v$  versus  $\delta_v$ ) as shown in Fig. 4. The  $F_v$  versus  $\delta_v$  relationship may be obtained using a modification to the procedures outlined by Schmertmann (1978). The iterative elastic procedure adopted to model the nonlinear soil behavior is as follows:

- (1) Divide the foundation soil layer into a number of sublayers (up to about four times the width of the foundation base)
- (2) For each layer, assume the initial secant shear modulus,  $G$ , to be a fraction of  $G_{max}$ . Here,  $G_{max}$  is the maximum shear modulus at a low shear strain; and it may be computed using the Seed and Idriss (1970) equation

$$G_{max} = 218.8(K_2)_{max}(\sigma_m)^{1/2} \quad (1)$$

in which  $(K_2)_{max}$  = the constant that depends on the relative density of the soil and  $\sigma_m$  = the mean normal stress of the layer. Here,  $G_{max}$  and  $\sigma_m$  are given in kPa and  $\sigma_m$  is computed using both components: the overburden and the load induced stresses. The average load induced stresses in the sublayer were computed using a 2:1 spread as often used in foundation engineering.

- (3) From the shear strains computed for the layers, estimate the secant shear modulus,  $G$ , using the variation routinely used in soil dynamics problems.
- (4) If the difference between the assumed (Step 2) and the computed shear modulus (Step 3) is not within a certain limit, repeat Steps 2 and 3. If convergence occurs in all sublayers, then the resulting settlement accounts for the nonlinear soil behavior.

The entire nonlinear vertical load-settlement ( $F_v$  versus  $\delta_v$ ) curve can be obtained by increasing the value of  $F_v$ . The curve is limited by the ultimate bearing capacity of the foundation as shown in Fig. 4.

### Earthquake Induced Inertia Forces and Free-Field Strains

The earthquake excitation shakes the bridge superstructure and also foundation and backfill soil surrounding the abutment. It may be argued that the strains in the surrounding soil have two components: free-field and strains from load applied at the abutment. This means that, since the soil is nonlinear, it is reasonable to expect that the abutment stiffness depends on the level of shaking. Since the dynamic characteristics of the superstructure and soil surrounding the abutment are quite different, the movement of the soil adjacent to the abutment will not be in phase with the bridge deck movement. When the bridge attempts to push into the abutment, there may be inertia forces present within the backfill and on the abutment. The analysis presented thus far neglects the influence of the inertia force. In fact, all of the current methods neglect the presence of inertia force. When inertia force is present, the maximum active and passive resistances for lateral movement are given by the Mononobe-Okabe equation (Seed and Whitman, 1970). Since the lateral earth pressure versus displacement curve adopted here is normalized, Mononobe-Okabe active ( $K_{AE}$ ) and passive coefficients ( $K_{PE}$ ) can be used with Fig. 2.

Since the excitation reverses in direction very often, the horizontal inertia forces could be

in a direction either to the left or to the right or even nonexistent when the deck attempts to move into the abutment. A similar situation exists with the vertical inertia force. Under these circumstances, it is herein proposed to evaluate abutment stiffnesses considering many possible combinations. The combinations that have been considered are horizontal seismic coefficient  $k_h = \pm 0.5 a_{\max}/g$ , the vertical seismic coefficient  $k_v = \pm k_h/2$ , and also  $k_h = k_v = 0$ . Here,  $a_{\max}$  is the maximum horizontal acceleration on top of the soil deposit and  $k_v$  has been assumed to be half of  $k_h$ . The selection of values for the seismic coefficient,  $k_h$ , had been based on the recommendation of Whitman (1991) who critically reviewed field observations in real earthquakes and laboratory tests. Altogether, there are five combinations; and, since the problem is nonlinear, it is not possible to predict beforehand which combination would yield the conservative results. It is believed that the cases with inertia forces and free-field strains and the case without earthquake excitation ( $k_v = k_h = 0$ ) can provide a bound for the stiffness evaluations.

The foundation and the backfill soil mass undergo deformation to the earthquake excitation (free-field). The free-field strains that are present due to earthquake shaking should be superimposed on the load induced strains for realistic nonlinear characterization (Lam and Martin, 1986; Buckle et al., 1987). The average free-field shear strains,  $\gamma_{eq}$ , in the foundation and backfill soil may be obtained as a function of depth using the procedures outlined by Tokimatsu and Seed (1987). This approach requires widely used soil properties such as  $(K_2)_{\max}$ , and unit weight,  $\gamma$  and  $a_{\max}$ . By superimposing the  $\gamma_{eq}$  on the load induced shear strain (Step 3 above), it is possible to account for the influence of the free-field strain on the stiffness estimation. Since both of the shear strain components are on two different perpendicular axes, they should not simply be added. Further, when inertia forces are considered, the bearing capacity of the foundation is reduced. Recent research reported by Richard et al. (1993) has been used to obtain the limit to the  $F_v$  versus  $\delta_v$  relationship.

## APPLICATION

To illustrate and highlight many important components of the proposed approach, many intermediate steps involved in the evaluation of the nonlinear stiffness of an abutment shown in Fig. 5 are presented. This is a medium high abutment with a height of  $H = 4.5\text{m}$  supporting a vertical deck load of  $V_D = 500\text{ kN/m}$ . This abutment has been designed according to the current design procedures (Barker et al., 1991) such that the factors of safety under static loading conditions against sliding, overturning, and bearing failures are more than 1.5, 2.0, and 2.0 respectively. Tension at the heel of the abutment is also not allowed to develop. In addition, this abutment has factors of safety under seismic loading conditions against sliding, overturning, and bearing failure of more than 1.1, 1.5, and 1.5 respectively. These factors of safety are consistent with those recommended in various design guidelines for abutment design (e.g., Barker et al., 1991; Siddharthan et al., 1994). A seismic coefficient,  $k_h = 0.2$  and  $k_v = 0.1$ , has been used in the pseudostatic design of the abutment. The backfill and foundation soil are assumed to have a friction angle of  $\phi_b = \phi_f = 35^\circ$ , and the interface friction angles at the base and on the side are assumed to be  $21^\circ$  and  $15^\circ$  respectively. These values are typical for medium dense sand and sandy silt mixtures (Barker et al., 1991). An optimization technique described by Siddharthan et al. (1994) was used to arrive at the abutment dimension at the base of the footing. Abutment dimensions (Fig. 5) and soil properties used are as follows:  $H = 4.5\text{m}$ ;  $H_p = 2.75\text{m}$ ;  $A_1 = 0.3\text{m}$ ;  $A_2 = 1.0\text{m}$ ;  $A_3 = 1.0\text{m}$ ;  $A_4 = 0.75\text{m}$ ;  $A_5 = 0.1\text{m}$ ;  $A_6 = 2.5\text{m}$ ;  $C_1 = 0.1\text{m}$ ;  $C_2 = 1.0\text{m}$ ;  $C_3 =$

4.25m;  $B = 3.9\text{m}$ ;  $\gamma = 18.5 \text{ kN/m}^3$ ; Poissons's ratio,  $\nu = 0.3$ ; and  $(K_2)_{\text{max}} = 55$ .

Figure 6 shows the vertical load-displacement ( $F_v - \delta_v$ ) relationship obtained for this abutment. Two cases are shown: (1)  $k_h = k_v = 0.0$  and (2)  $k_h = 0.2$  and  $k_v = 0.1$ . The limiting vertical load given by the bearing capacity equations with  $k_h = 0.2$  is much smaller and is as much as 0.3 of the limiting vertical load when  $k_h = 0$ . The  $F_v - \delta_v$  relationship developed for  $k_h = 0.2$  required a knowledge of free-field strains. The procedures adopted by Tokimatsu and Seed (1987) were used to estimate the average free-field shear strains. Figure 7 presents this variation. These strains were superimposed with the load induced strains to obtain the  $F_v - \delta_v$  relationship for the case where  $k_h = 0.2$ . It may be noted that the nonlinear behavior is present from the start and the ultimate bearing pressures is reached in the cases of  $k_h = 0.2$  much sooner after the vertical displacement of 7mm; while, in the case of  $k_h = 0.0$ , as much as 72mm displacement is required. It appears that there is no major difference between the cases  $k_h = 0$  and  $k_h = 0.2$  until the ultimate bearing resistance is reached with the  $k_h = 0.2$  case.

Figure 8 presents the longitudinal secant stiffness evaluated using the procedures outlined above. The figure depicts five cases. In all of the cases reported in the figures, it is clear that the stiffness drops substantially, by as much as a factor of 9, when the displacement increases from 1 to 10mm. Such reduction in stiffness is consistent with the recent large-scale field test results reported by Maroney et al. (1994). In all cases, after about 20mm of movement, there is not much change in the stiffness. Figure 9 shows a range for the stiffnesses. The case of  $k_h = 0.2$  and  $k_v = 0.1$  always represents the upper bound (stiffer) data, while the case of  $k_h = k_v = 0$  represents the lower bound (softer) data. The highest deviation between the five cases exists at a lower displacement; and it can be as much as 18%.

In design, it is often customary to select the lower abutment stiffness. This is because lower abutment stiffness will usually produce higher displacements for the deck and the pier and, therefore, lead to higher ductile demand and shear forces in the pier. However, in an extreme case when an iterative elastic bridge response analysis is performed, the softer springs can change the dynamic characteristics (period and mode shapes) and, thus, result in an unrealistic analytical model. Since the variations shown between the different cases are within 18%, the influence of this on altering the effective period of the entire bridge structure will be minimal.

## REFERENCES

- Applied Technology Council. 1978. *ATC-3-06 Tentative Provisions for the Devel. of Seis. Regs. for Bldgs.*
- Barker, R.M., Duncan, J.M., Rojiani, K.B., Ooi, P.S.K., Tan, C.K., and Kim, S.G. 1991. Manuals for the design of bridge foundations. NCHRP Rep. 343, Transportation Research Board, Washington D.C.
- Buckle, I.G., Mayes, R.L., and Button, M.R. 1987. Seismic Design and Retrofit Manual for Highway Bridges. Report No. FHWA IP-87-6, FHWA, Washington D.C.
- Clough, G.W., and Duncan, J.M. 1991 *Foundation Engrg. Hndbk.*, 2nd Edition, edited by H.Y. Fang, Van Nostrand Reinhold, New York, NY, 223-235.
- Lam, P.L., and Martin, G.R. 1986. seismic Design of Highway Bridge Foundations. Report No. FHWA RD-86-101, FHWA, Washington D.C.

- Maroney, B., Kutter, B., Romstad, K., Chai, Y.H., and Vanderbilt, E. 1994. Interpretation of Large Scale Bridge Abutment Test Results. 3rd Annual Seismic Research Workshop, CalTrans, Sacramento, CA.
- Maragakis, E.A., and Siddharthan, R. 1989. A Simple Model for Estimation of the Nonlinear Abutment Stiffness in the Longitudinal Direction. *J. of Struct. Engr.*, ASCE, Vol. 115(9), 2382-2398.
- Richards, R., Elms, D.G., and Budhu, M. 1993. Seismic Bearing Capacity and Settlements of Foundations. *J. Geotech. Engrg.*, ASCE, Vol. 119(4), 662-674.
- Schmertmann, J.H., Hartman, J.P., and Brown, P.R. 1978. Improved Strain Influence Factor Diagrams. *J. Geotech. Engr.*, ASCE, Tech. Notes, Vol. 104(8), 1978, 1131-1135.
- Seed, H.B., and Idriss, I.M. 1970. Soil Moduli and damping in Soils, Design Equation and Curves. Rep. No. EERC 70-10, Earthquake Engrg. Research Center, University of California, Berkeley.
- Seed, H.B., and Whitman, R.V. 1970. Design of Earth Retaining Structures for Dynamic Loads. Specialty Conf. on Lateral Stresses in Ground and Design of Earth Retaining Struct., ASCE, New York, 103-147.
- Siddharthan, R., Ara, S. and Norris, G.M. 1992. Simple Model for Rigid Plastic Model for Seismic Tilting of Rigid Walls. *J. of Struct. Engr.*, ASCE, Vol. 118(2), 469-487.
- Siddharthan, R., El-Gamal, M., and Maragakis, E.A. 1994. Investigation of Performance of Bridge Abutments in Seismic Regions. *J. of Struct. Engr.*, ASCE, Vol. 120(4), 1327-1346.
- Tokimatsu, K., and Seed, H.B. 1987. Evaluation of Settlement in Sands due to Earthquake Shaking. *J. of Geotech. Engr.*, ASCE, Vol. 113(8), 861-878.
- Whitman, R.V. 1991. Seismic Design of earth Retaining Structures (State-of-the-Art Paper). Proc. 2nd Conf. on Recent Adv. in Geotech. Earthquake Engrg., St. Louis, Mo., Vol. II, 1,767-1,778.
- Wilson, J.C., and Tan, B.S. 1990. Bridge Abutments: Formulation of Simple Model for Earthquake Response Analysis. *J. of Engr. Mechanics*, ASCE, Vol. 116(8), 1828-1856.
- Yu, G., Anderson, J.G., and Siddharthan, R. 1993. On the Characteristics of Nonlinear Soil Response, *Bull. Seism. Soc. Am.*, Vol. 83, 218-244.

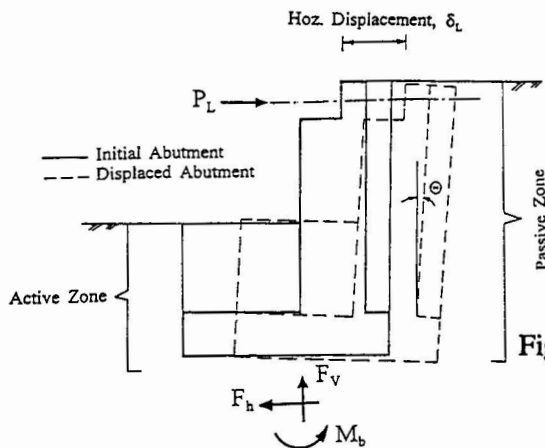


Fig. 1: Sketch of Displaced Abutment Caused by a Longitudinal Force.

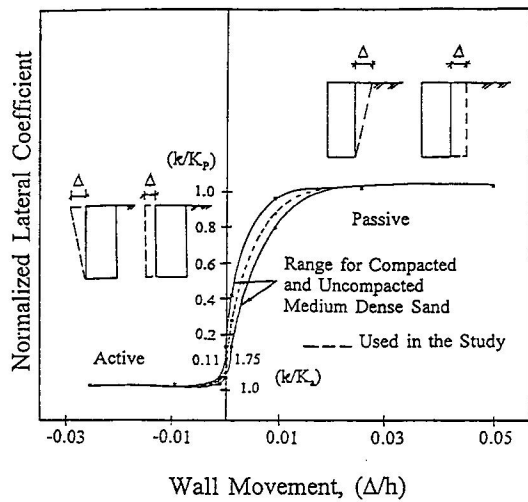


Fig. 2: Normalized Lateral Wall Pressure-Displacement Relationship (After Clough and Duncan, 1991).

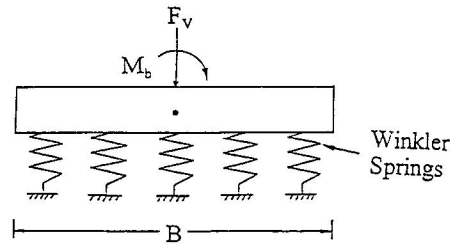


Fig. 3: Winkler Spring Representation for Abutment Base.

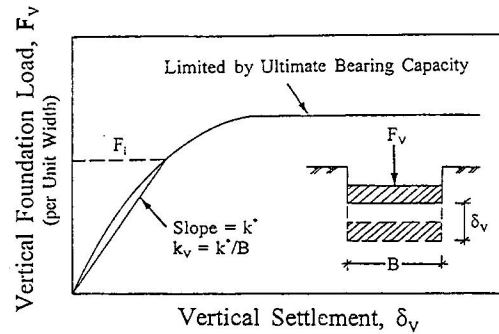


Fig. 4: Typical Nonlinear  $F_v$ - $\delta_v$  Relationship.

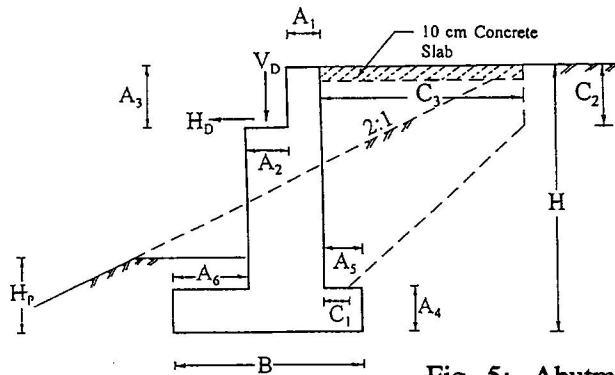


Fig. 5: Abutment Dimensions

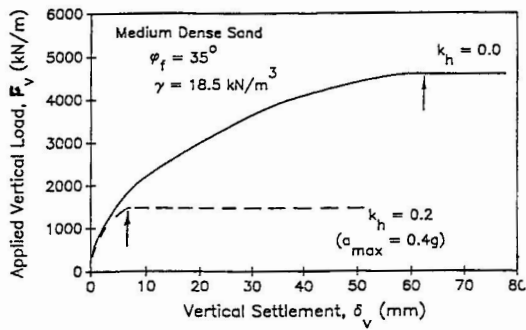


Fig. 6:  $F_V$ - $\delta_V$  Relationship at the Abutment Base.

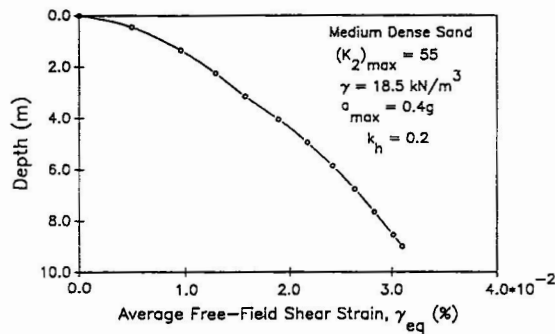


Fig. 7: Free-Field Shear Strains from Tokimatsu and Seed (1987) Procedure.

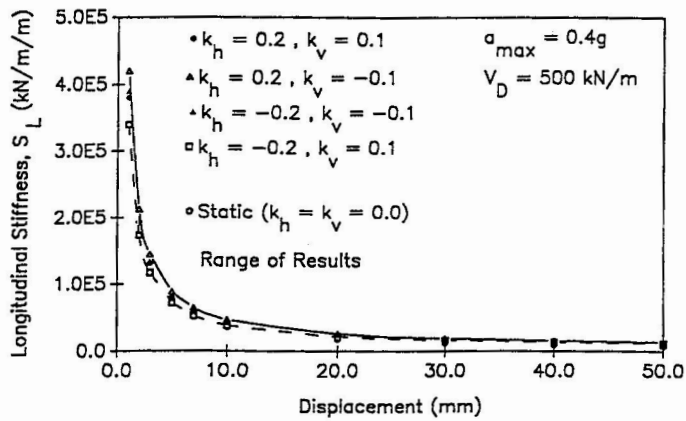


Fig. 8: Secant Longitudinal Stiffnesses for all Cases.